RAPID COMMUNICATIONS

PHYSICAL REVIEW C VOLUME 41, NUMBER 1 JANUARY 1990

Critical excitation energy in fusion-evaporation reactions

W. Bohne, H. Morgenstern, K. Grabisch, T. Nakagawa,* and S. Proschitzki
Hahn-Meitner-Institut Berlin GmbH, Bereich Kern- und Strahlenphysik, 1000 Berlin 39, Germany
(Received 24 February 1989; revised manuscript received 23 August 1989)

The widths of the residue-mass distributions are used as a measure of the excitation energy of hot nuclei. They increase with the recoil velocity but saturate much below the calculated velocity v_{CN} for complete fusion. Above these critical excitation energies (4.5–6.4 MeV/nucleon) derived from the recoil velocity, the normal evaporation of nucleons and small clusters disappears, if a hot and equilibrated compoundlike nucleus is formed at all.

Fusion reactions with heavy ions at intermediate bombarding energies are a good tool to create nuclei at high excitation energies. Complete fusion is no longer the dominant channel. Incomplete fusion reactions lead to different compound nuclei with a broad range of excitation energies. Experimental[1–3] and theoretical investigations[4–13] predict that nuclei cannot endure excitation energies per nucleon ϵ^* above a certain limit ranging between 3 and 8 MeV/nucleon. On the average this value of about 70% of the total binding energy per nucleon is expected as "critical excitation energy" of hot nuclei. Above this limit phenomena such as multifragmentation should preferentially contribute to the nuclear disintegration. Some experiments[14–17] in this energy range seem to indicate that indeed fusionlike reactions do not occur anymore, or at least are not detectable anymore via the normal decay modes. A usual experimental method to extract the critical excitation energy exploits the excitation function of the decreasing cross section for fusionlike reactions with increasing incident energy. We present a new experimental method to obtain values for this critical excitation energy for medium mass compound nuclei at each incident energy separately.

From our systematic study of incomplete fusion[18] we know that the fraction of complete fusion decreases almost linearly with increasing c.m. velocity v_L of the lighter reaction partner A_L up to the extrapolated limit of $v_L \approx 0.19c$ (c denotes velocity of light) above which complete fusion ceases to exist. This value corresponds to an excitation energy per nucleon of the compound nucleus of $\epsilon^*_{\rm lim} \approx A_L/A_H\, 17$ MeV/nucleon. In our experiment we have chosen the asymmetry of the systems and the incident energies in a way that the excitation energies per nucleon for complete fusion are much below this predicted entrance channel limitation. On the other side the excitation energies per nucleon for complete fusion and some incomplete fusion channels with the highest linear momentum transfer should be large enough to examine the above cited critical value. To determine the total excitation energy deposited in a compound nucleus the kinetic energies of all outgoing particles and γ rays should be measured. Such a complete experiment is, as far as we know, not yet performed. Therefore we try to extract at least some averaged values of this quantity from higher moments of precisely measured inclusive evaporation residue (ER) mass distributions. The idea is simple. The more complete the process is the higher the excitation energy of the corresponding compound nucleus should be. As a consequence, the number of evaporated light particles should also increase. For neutrons this is observed by Galin.[19] But the mass centroid as a function of the ER velocity is not a very helpful quantity to learn something about the fusion-reactions mechanism, because the nonfusing fractions Δm_P and Δm_T of the projectile m_P and target m_T, respectively, are not well known. The decay of these hot compound nuclei is not very precisely established as well. In the mass region studied, the ratio of the competing decay channels $(n,p,\alpha,\ldots)$ may fluctuate somewhat for the different compound nuclei formed by the various incomplete fusion components. The estimated numbers of evaporated particles are based on extrapolations from lower excitation energies. While the gain of excitation energy per additional mass unit of the fusing projectile fraction is a decreasing function for increasing ER velocity v_R, i.e., increasing momentum transfer,[20] the averaged amount of excitation energy carried away per evaporated mass unit is assumed to be a constant or slowly increasing function with increasing excitation energy[21] depending on the mass of the compound nucleus. Therefore the mass centroid varies with increasing velocity v_R. The absolute values and even the slope of the first moment as a function of v_R depend on the mass asymmetry of the system and on the beam energy and are not very well established (see, e.g., Hagel *et al.*[22]).

But the increasing excitation energy causes an increasing width of the ER mass distribution. For each fusion channel the mass width is constant for a certain ER velocity interval Δv which is populated symmetrically around the averaged velocity v_{CN}, by the kinematics of the decay cascade. We confirmed this behavior experimentally in the case of the "inverse" fusion reaction ^{58}Ni+^{27}Al at $E(^{58}\text{Ni}) = 580$ MeV which forms one complete compound nucleus very similar in mass and excitation energy ($\epsilon^*_{CN} = 2.0$ MeV/nucleon) to those populated by the incomplete fusion channels of the discussed reactions at higher energies. For these energies we performed evaporation calculations (code JULIAN) which also show constant mass widths for the main part of the cross section. The intensity weighted sum σ_A of the mass widths of all contributing fusion channels does not exhibit the behavior of a step function, but increases steadily with increasing v_R (in the case of normal kinematics) until it reaches a constant

value corresponding to the excitation energy of the last contributing fusion channel. (This expected behavior is also confirmed by JULIAN evaporation calculations; see below.) Due to the width of each velocity distribution, this is not a sharp transition. The mean velocity of this last fusion channel is located approximately in the middle of this transition region and should reach the value of complete fusion v_{CN} for all reactions we have measured. The uncertainty of the determination of this mean velocity value depends on the widths and the shift of the last two contributing velocity distributions.

Using the simple framework of a participant-spectator model where the nonfusing parts Δm_P and Δm_T of the projectile m_P and target m_T remain cold and keep their initial velocities v_P and v_T, respectively, and taking into account energy and momentum conservation, the calculation of the total excitation energy per nucleon results in $E^*/m_R = \epsilon^* = \frac{1}{2}(v_P - v_R)v_R + Q_{gg}/m_R$, where Q_{gg} is the mass balance of the reaction and $m_R = m_P + m_T - \Delta m_P - \Delta m_T$ the compound mass. Thus ϵ^* depends only on the residue velocity v_R neglecting the corresponding Q value, which is small compared to the first term. Unfortunately, nature is not so simple. The coincidence experiments show (see below) that the assumptions of the participant-spectator model are not strictly true. The nonfusing fractions of projectile and target do not keep their initial velocities and directions. Furthermore, they carry away some excitation energy themselves. Therefore, the whole excitation energy of the system is given by

$$\epsilon^* = \tfrac{1}{2}(\cos\theta_R v_P - v_R)v_R + Q_{gg}/m_R + \tfrac{1}{2}\Delta m_P/m_R(\cos\theta_P v_P - v_{P'})v_{P'} + \tfrac{1}{2}\Delta m_T/m_R(\cos\theta_T v_P - v_{T'})v_{T'}, \quad (1)$$

where $v_{P'}$ and $v_{T'}$ are the final velocities of the nonfusing parts Δm_P and Δm_T, respectively, θ_P, θ_T, and θ_R are the corresponding angles relative to the beam axis. In general the unknown nonfusing fractions Δm_P and Δm_T must not necessarily be one piece; therefore, the last two terms in Eq. (1) have to be replaced by sums. However, Δm_P and Δm_T are much smaller than m_R and since the final velocity $v_{P'}$ is not so different from the initial v_P and since $v_{T'}$ is small, the last two terms are relatively small compared to the first one. This method gives the total energy transferred from initial relative motion into other degrees of freedom, i.e., the excitation energy or deposited energy. We are not going to discuss whether it is only thermal energy or if it may also include some compressional and rotational energy. This is done in detail by Peter and Tamain[23] and by Fabris *et al.*[17] Since not all of this energy is necessarily transformed into thermal energy the measured excitation energy per nucleon is an upper limit of the temperature.

The experiments were performed with ^{32}S beams of 960, 840, and 710 MeV from the heavy-ion accelerator VICKSI. We used rolled self-supporting targets made from highly enriched ^{45}Sc, ^{51}V, ^{58}Fe, and ^{58}Ni with thicknesses between 0.5 and 1 mg/cm^2. The residues have been measured with the time-of-flight method, using a new type of a gridless channel-plate start detector.[24] The flight path between this detector and a surface-barrier stop detector was about 1 m, the total time resolution amounted to about 60 ps. At the opposite side relative to the beam direction light projectilelike ions were identified by means of normal $\Delta E - E$ technique with surface-barrier detectors. The energy-loss detector was 65 μm thick and allowed to resolve the elements up to S. All measured energies and times were corrected for ionization defect[25] and plasma delay.[26] In all measurements the achieved mass resolution is good enough to obtain velocity spectra of clearly separated masses as shown in Fig. 1 for the more difficult case at low incident energy. This is absolutely necessary in order to be sure, that one has parallel velocity spectra for all masses to obtain reliable values of the mass centroids and of the mass widths at different velocities. The events at small velocities ($v_R < 1$ cm/ns) due to targetlike recoils of inelastic reactions have not been subtracted because they do not have any effect on the results at the interesting velocity of about 2 cm/ns.

From these spectra we created mass distributions for small velocity intervals ($\Delta v = 0.05$ cm/ns). At higher velocities and for masses lighter than the one with maximum intensity one has to be aware of disturbing contaminations due to deep inelastic and/or fusion-fission events. In the similar reaction ^{40}Ar + ^{68}Zn at comparable energies[3] the fusion-fission fraction amounts to about 40% of the total fusion cross section. For the ^{32}S + ^{58}Ni reaction JULIAN evaporation calculations predict only a contribution of 10% to 20%. In addition, ER's are favored at small forward angles. Nevertheless, we do not take into account the light-mass region below $\frac{1}{2}A_{CN}$ to determine σ_A. We used normal distributions to extract the variances of the mass distributions although JULIAN calculations do not show perfect Gaussians. (Different procedures to extract the mass width, e.g., without using normal distributions, alter the absolute values of σ_A but do not change the general shape of the curves.) We extracted width functions for all targets and energies used. In Fig. 2 we display the

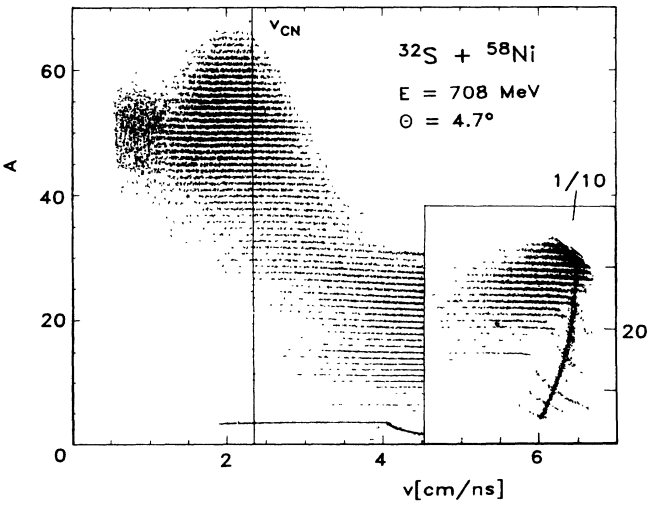

FIG. 1. Mass vs velocity spectrum of the fusion reaction ^{32}S + ^{58}Ni at 22 MeV/nucleon. The vertical line v_{CN} gives the velocity centroid for complete fusion.

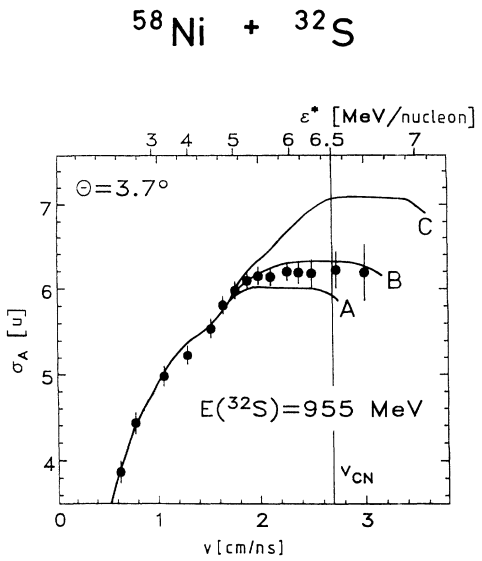

FIG. 2. Mass widths of evaporation residues from the reaction $^{32}S+^{58}Ni$ as a function of the residue velocity (lower axes). The upper axes refer to the excitation energy per nucleon of the corresponding compound nuclei. The curves *A*, *B*, and *C* represent results of evaporation calculations including all incomplete fusion channels with ^{16}O, ^{20}Ne, and ^{32}S as heaviest fusioning projectile, respectively (see text).

result for the ^{58}Ni target. All the other cases show a similar behavior: a steep rise with increasing velocity and a transition to saturation at velocities $\tilde{v}_R$ much below the maximum possible one, v_{CN}, for complete fusion. It should be noted that this saturation does not occur at the velocity where the cross section is maximum. Corresponding results, a saturation of the proton- and α-multiplicities much below the maximum possible excitation energy for complete fusion in the case of Ar+Ag at 39 and 60 MeV/nucleon were presented recently.[27]

To support our qualitative description of the expected ER mass width, given above, we performed a series of evaporation calculations (code JULIAN) for the 30 MeV/nucleon data with the following assumptions. All incomplete fusion channels up to complete fusion can contribute. But only the "α-like" channels $^{58}Ni+\alpha$, ^{8}Be, $^{12}C \cdots ^{32}S$ were calculated. The different fusion channels were weighted according to a normal distribution with a sum equal to the measured total ER cross section (≈ 300 mb) and a fraction of complete fusion ($\approx 20\%$) according to our systematics.[18] The excitation energies of the compound nuclei formed by the various incomplete fusion channels were also assumed to have normal distributions with widths estimated from the measured energy distributions of the corresponding spectator particles. The mean velocity $v_{P'}$ of all these light ions with $3 \leq Z \leq 10$ amounts to (90–95)% of the beam velocity. The remaining amount of energy was shared between the fusing parts of the projectile and the spectators according to their mass ratios. (This does not influence the shape of the mass-width function considerably but decreases the first moments of the mass distribution.) Three examples of these calculations, representing the sum of all contributions up to $^{58}Ni+^{16}O$, $^{58}Ni+^{20}Ne$, and up to complete fusion, are displayed as curves in Fig. 2, labeled *A*, *B*, and *C*, respectively. To fit the steep rise of the data we have to increase all calculated width functions by almost 50%. This may be related to the disregarding of all more complex incomplete fusion channels and to the restriction of the evaporation particles (only *n*, *p*, *d*, and α were allowed). The best fit we would obtain with a maximum fusing projectile fraction of mass 18. Taking into account the different possible values of Q_{gg}, this results in a maximum excitation energy per nucleon of about (5.6 ± 0.3) MeV/nucleon.

Now we calculate the excitation energy per nucleon according to Eq. (1). To do so we use again the results of the coincidences between evaporation residues and fast-forward-emitted projectile fragments. The angular distribution is very strongly forward peaked. The mean angle should be smaller than $\theta_P \approx 10°$. Similar assumptions in the corresponding c.m. system are made for the nonfusing fractions Δm_T which are not detectable due to their small velocities. For selected nuclei of the nonfusing fractions Δm_P and Δm_T, e.g., *p*, *n*, *d*, *t*, ^{3}He, ^{4}He, . . . , we calculate the recoil velocity v_R, the recoil angle θ_R, the corresponding Q_{gg} value, and finally the total excitation energy per nucleon ϵ^* with Eq. (1). From a smooth curve, fitting these fluctuating calculated values, we obtain the averaged excitation energy for different momentum transfers. The mean deviations from this curve are included in the uncertainties of the results given in Table I. But the major contribution to the uncertainty is due to the difficulties to determine $\tilde{v}_R$, the center of the transition region, because one additional mass unit of the fusing projectile fraction results in a small shift less than 0.1 cm/ns of the corresponding velocity distribution whereas the half-width at noticeable cross section is about 0.3 cm/ns. These excitation energies may be somewhat too high, because we know from the coincidence data that the assumption of cold emitted nonfusing fragments is not correct. The measured mean velocity of all evaporation residues in coincidence with fast fragments of a certain *Z* is too small compared to the calculated one. To bring these values into accord we have to assume a somewhat heavier (about four mass units) nonfusing fraction decaying sequentially

TABLE I. Maximum and critical excitation energies.

Projectile ^{32}S energy (MeV)	Target	ϵ^*_{CN} (MeV/nucleon)	$\tilde{v}_R$ (cm/ns)	ϵ^*_{crit} (MeV/nucleon)
955	^{45}Sc	7.2	2.4 ± 0.2	6.3 ± 0.4
	^{51}V	6.9	2.5 ± 0.2	6.4 ± 0.4
	^{58}Ni	6.5	2.0 ± 0.2	5.4 ± 0.4
836	^{58}Ni	5.7	2.1 ± 0.2	5.1 ± 0.3
708	^{45}Sc	5.3	2.6 ± 0.2	5.2 ± 0.3
	^{51}V	5.2	2.4 ± 0.2	5.1 ± 0.3
	^{58}Fe	5.0	2.2 ± 0.2	4.9 ± 0.3
	^{58}Ni	4.8	2.0 ± 0.2	4.5 ± 0.3

to the mass of the detected one. With all these small corrections we obtained from the velocities $\tilde{v}_R$ the maximum or critical excitation energy per nucleon, which the compound nuclei display. The results for the different measured systems are listed in Table I, together with calculated maximum possible values ϵ^*_{CN} for complete fusion. The agreement with the result obtained from the JULIAN calculation is good. According to our systematics[18] the fraction of complete fusion is expected to be about 20% at 30 MeV/nucleon incident energy and about 40% at 22 MeV/nucleon. These are no negligible cross sections. If they contribute to the formation of ER's the described method should be able to detect this. Thus the measured saturation of σ_A at excitations below that of the completely fused system is a significant result and seems to indicate a limitation for the survival of ER's in addition to the known entrance channel limitations of momentum/energy transfer as expressed by our systematics.[18]

The results listed in Table I for limiting ϵ^* are in good agreement with values for this compound nucleus mass region obtained by other experimental methods (see e.g., the compilations of Refs. 15 and 23). They are also in the order of the theoretically predicted 70% of the total binding energy.[11] The variations due to the different targets are larger than the experimental uncertainties, but cannot be described as a mass dependence. A qualitative explanation of these differences is provided by the calculations of Refs. 6 and 10, which take into account the charge-to-mass ratio of the formed compound nucleus. Starting with the Ni target we will reach compound nuclei with the highest Z to N ratios, always assuming that the light nonfusing fractions on the average have equal numbers of protons and neutrons. That means, these nuclei have a larger distance to the β-stability line and can stand less excitation energy. The same argument holds also for the decreasing values of ϵ^*_{crit} at lower bombarding energies, because the fusion cross section is shifted to more complete fusion channels. These heavier compound nuclei also move away from the stability line.

To prove the theoretical predictions and to corroborate the difference of the excitation energy borderline from that of the momentum transfer limitation concerning the dependence on the mass and Z/N ratio of the compound nucleus, more measurements on lighter and heavier systems and especially with extremely distant isobaric target nuclei are necessary.

---

*Present address: The Institute of Physical and Chemical Research (RIKEN), Linac Laboratory, Hirosawa 2-1, Wako-shi, Saitama 351-01, Japan.

[1]M. Lefort, Nucl. Phys. **A387**, 3c (1982).
[2]H. Nifenecker *et al.*, Nucl. Phys. **A447**, 533 (1985).
[3]A. Fahli *et al.*, Phys. Rev. C **34**, 161 (1986).
[4]J. P. Bondorf, Nucl. Phys. **A387**, 25 (1982).
[5]X. Campi, J. Desbois, and E. Lipparini, Nucl. Phys. **A428**, 327 (1984).
[6]S. Levit and P. Bonche, Nucl. Phys. **A437**, 426 (1985).
[7]J. Bondorf, R. Donangelo, I. N. Mishustin, and H. Schulz, Nucl. Phys. **A444**, 460 (1985).
[8]D. H. E. Gross, Zhang Xiao-ze, and Xu Shu-yan, Phys. Rev. Lett. **56**, 1544 (1986).
[9]J. Desbois, O. Granier, and C. Ngô, Z. Phys. A **325**, 245 (1986).
[10]E. Suraud, Nucl. Phys. **A462**, 109 (1987).
[11]J. Desbois, R. Boisgard, C. Ngô, and J. Nemeth, Z. Phys. A **328**, 101 (1987).
[12]H. W. Barz, J. P. Bondorf, and H. Schulz, Phys. Lett. B **184**, 125 (1987).
[13]C. Cerruti *et al.*, Nucl. Phys. **A476**, 74 (1988).
[14]B. Borderie and M. F. Rivet, Z. Phys. A **321**, 703 (1985).
[15]S. Leray, J. Phys. (Paris) Colloq. **47**, C4-275 (1986), and references therein.
[16]M. Lefort, J. Phys. (Paris) Colloq. **47**, C4-427 (1986).
[17]D. Fabris *et al.*, Phys. Lett. B **196**, 429 (1987).
[18]H. Morgenstern *et al.*, Phys. Rev. Lett. **52**, 1104 (1984).
[19]J. Galin, Nucl. Phys. **A447**, 519 (1985).
[20]H. Morgenstern *et al.*, Phys. Lett. **113B**, 463 (1982), and references therein.
[21]A. Y. Abul-Magd, W. A. Friedman, and J. Hüfner, Phys. Rev. C **34**, 113 (1986).
[22]K. Hagel *et al.*, Nucl. Phys. **A486**, 429 (1988).
[23]J. Peter and B. Tamain, Report No. Ganil P-87-24, Grand Accélérateur National d'Ions Lourds, 1987 (unpublished).
[24]T. Nakagawa and W. Bohne, Nucl. Instrum. Methods Phys. Res. Sect. A **271**, 523 (1988).
[25]S. B. Kaufmann *et al.*, Nucl. Instrum. Methods **115**, 47 (1974).
[26]W. Bohne, W. Galster, K. Grabisch, and H. Morgenstern, Nucl. Instrum. Methods Phys. Res. Sect. A **240**, 145 (1985).
[27]G. Bizard *et al.*, in *Proceedings of the Texas A&M Symposium on Hot Nuclei,* edited by S. Shlomo, R. P. Schmitt, and J. B. Natowitz (World Scientific, Singapore, 1988), p. 262.